

## **1. Introduction**

When one looks at the Moon through binoculars or a small telescope, some of the most apparent features are the craters that dominate much of its landscape. Impact craters are prevalent across the surface of almost every solid body in the solar system; the notable exceptions are Earth, Titan, Io, and regions of Triton and Enceladus where rapid, ongoing resurfacing is caused by endogenic processes. Venus also presents an abbreviated crater pattern due to volcanic resurfacing and a thick atmosphere that prevents many smaller impactors from reaching the planet's surface. On bodies that lack active resurfacing, impact craters are the primary mode of surface modification, both in the present and even more so in the past. A single impact likely formed our Moon and gave Earth a disproportionately large iron core. Impacts deliver water, and they may also deliver organic compounds like amino acids to planets, helping life to begin. Conversely, a large impact can completely destroy life that has formed. Impacts on Earth have been tied to some of the greatest extinction events in our planet's history, and future impacts may repeat this.

Understanding impactor and crater populations is a key part of understanding the history of the solar system. From the initial collisions that formed the planets to the continued impacts today, knowing the impactor population and flux through time is integral to interpreting the geologic past and its processes. Because crater sizes relate to the object that formed them, comprehensive studies of crater populations inform impactor population censuses. Craters can be used to determine relative surface ages, resurfacing rates, and properties of the crust within which they form. Differences in impact crater morphology from an expected norm can be used to glean further information about the surface and near-surface properties that modified them. Studying actual impacts also puts constraints on models of crater formation. This is important for understanding the underlying physics of such destructive events, ranging from natural incidents by asteroids and comets to manmade affairs by bombs and missiles. Delving into these issues and questions forms the bulk of this dissertation, but in order to understand how

differences among craters inform these applications, one must first understand the basics of impactor populations, crater formation, and crater morphology.

### **1.1. Crater Production Throughout the Solar System's History**

The cratering rate and number of craters of a given size on the solar system's bodies are dependent almost entirely upon the number of potential impactors. Projectiles in the inner solar system are, for the most part, asteroids disrupted from the asteroid belt. To a lesser extent, comets will also impact planets (*e.g.*, Comet Shoemaker-Levy 9's collision with Jupiter in 1994), though their role in cratering during the lifetime of the solar system has been debated (*e.g.*, Levison *et al.*, 2001; Ivanov, 2001). The discussions and calculations in this work are based upon asteroid-only models. The role of comets is contested, but if they play a role, it is believed they mainly follow the same trends seen in asteroids (see Melosh, 1989; Neukum *et al.*, 2001). Their inclusion would change the nature of the impactors, but in the inner solar system it should not significantly affect important variables such as the average size- and impact velocity-distributions. In the outer solar system, comets likely play a much more significant role and their population should not be averaged out.

Today, most asteroids lie between the orbits of Mars and Jupiter in the Main Asteroid Belt. Their size distribution is governed by collisions which yield the theoretical "production function" size-frequency distribution (Ivanov, 2001). This can be compared observationally with crater sizes on planets (Melosh, 1989). This distribution is such that when a histogram of diameters integrated from large to small sizes is graphed logarithmically, the slope is  $b \approx -3$ . A fit to the current data on asteroids yields a -3.3 slope (data for 547,100 asteroids, downloaded on March 14, 2011, from Lowell Observatory). Asteroids are also found in other parts of the solar system and can cross planetary orbits, but such asteroids are much fewer in number than the Main Belt asteroid population (~2% of identified asteroids).

Based upon the established lunar timescale (*e.g.* Neukum *et al.*, 2001) (see Fig. 1), the cratering rate just after the solar system's formation ~4.5 Ga ago was up to  $10^5$  times today's rate,

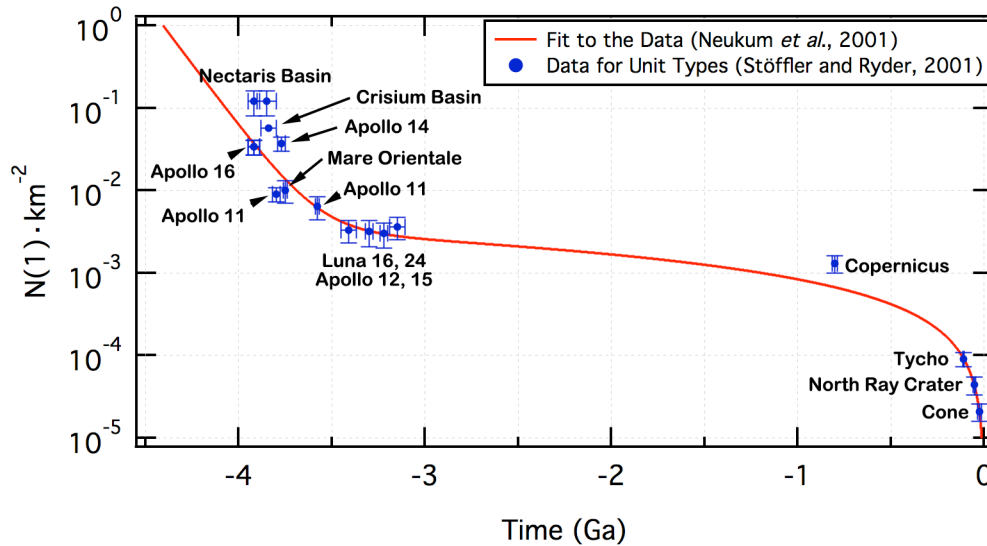


**Figure 1:** Cratering rate through the solar system's history. Vertical axis is the number of craters that are  $D \geq 1$  km per  $\text{km}^2$ , and the horizontal axis is billions of years before the present. Function is Eq. 5 from Neukum *et al.* (2001) and data and uncertainties are from Table VI from Stöffler and Ryder (2001). An  $N(\#)$  age is an age based upon the number of craters per unit area that are greater than or equal to the parenthetical number.

or up to  $10^6$  1-km craters per  $10^6 \text{ km}^2$  per Ga. This rate exponentially decayed until  $\sim 3.5$  Ga ago, at which time the cratering rate was  $\sim 3 \times 10^2$  times greater than what it is today, or  $3 \times 10^3$  1-km craters per  $10^6 \text{ km}^2$  per Ga. From then until about the time Copernicus Crater was formed ( $\sim 1$  Ga ago on the Moon), the impactor flux decreased slowly to  $\sim 10^2$  today's rate. Over the last billion years, the flux continued to decay dramatically, down to the current estimated rate of 10 1-km craters per  $10^6 \text{ km}^2$  per Ga. With high-resolution imagery repeatedly gathered over several years for Mars and the Moon, directly measuring the present-day impact flux can now be estimated (*e.g.*, Malin *et al.*, 2006; Daubar *et al.*, 2010, 2011).

It has been argued lately (*e.g.*, Neukum, 2001) that the size distribution of asteroids has remained constant through time, or at least for the last 4 Ga. This certainly makes extrapolation of historic crater populations easier, but it also was not necessarily true during the very early part of the solar system's history (*e.g.*, Strom *et al.*, 1992, 2008). The difference is that today's function is governed by collisional processes among the impactor population while, early in the solar system's history, potential impactors had not had time to break down via collisions to form the size distribution presently observed. Rather, according to some models, their size

distribution would be more closely linked to accretionary growth during the solar system's formation (*e.g.*, Strom *et al.*, 1992, 2008). For simplicity, however, Hartmann and Neukum (2001) and Hartmann (2005) adopt the position of a consistent production function when establishing the Martian isochrons (isochrons are established crater frequencies as a function of diameter for a given surface age; see Sections 1.4.1, 5.2.4).

This earliest period of heavy cratering is aptly named the "Heavy Bombardment," while a subsequent period ~700 Ma later saw a pulse of increased cratering termed the "Late Heavy Bombardment" (LHB). This was possibly caused by dynamic interplay between the large gas and ice giant planets – Jupiter, Saturn, Uranus, and Neptune (*e.g.*, Gomes *et al.*, 2005) (described as the "Nice Model"). This period is significant for all terrestrial bodies in the inner solar system, not only because the relatively frequent impact rate pulverized their surfaces, but also because *most* of the craters that would ever be carved out of the landscape were formed during this period of time. The Heavy Bombardment was also an important time because most of the largest asteroid impacts in our solar system occurred during that period, forming the large lunar basins, Mercury's Caloris Basin, and basins such as Mars' Utopia, Isidis, Hellas, and Argyre (Nimmo and Tanaka, 2005). Post-LHB impactors may have originally been seeded from the asteroid belt, but their population derives from inner solar system –crossing asteroids and comets.

## **1.2. Crater Formation**

Primary exogenic craters form during hypervelocity (10s of km/sec) impacts of a projectile into a planetary surface. Because of impactors' high velocities, the initial shape of the projectile and angle of impact (except for very low angles) will not significantly affect the final crater morphology. Velocities of asteroidal impactors are typically between 10-20 km/sec in the inner solar system (McEwen and Bierhaus, 2006), though these velocities increase closer to the Sun and so are less at Mars than Earth. The following discussion is primarily adapted from Melosh (1989).

There are three main stages of crater formation; the divisions are artificial but aid in the understanding the cratering process. The first stage is contact and compression, wherein the projectile physically contacts the target's surface. This compresses both the impactor and the surface as the impactor burrows into the target, moving material in the process. Most of the kinetic energy from the projectile is transferred into the target. Shock pressures typically reach hundreds of GPa (similar to the pressure of the metallic hydrogen layer in Jupiter's atmosphere) which easily exceeds the yield strength of both the projectile and target, causing them to deform, melt, and/or vaporize. This stage ends when the projectile is destroyed by shock waves.

The second stage is excavation wherein the transient crater cavity forms. The shock and subsequent rarefaction waves that travel through the target physically move the target material in a process that eventually opens the crater to a size many times the projectile's initial diameter (this is one of the primary differences between low-velocity and hypervelocity impacts). The target's gravity takes a more important role in the cavity's formation during this phase. The crater will initially be excavated to a depth  $\sim 3$  times its final depth, which is  $\sim 30\%$  the transient diameter regardless of final simple or complex morphology. For simple craters, the transient diameter is  $\sim 85\%$  the final diameter, and for larger complex craters, it is  $\sim 50-65\%$  the final diameter (these morphologies are discussed in Section 1.3); it is smaller than the final cavity due to slumping that occurs during the next stage. During this stage, most of the ejecta is deposited: Jets of still-solid, melted, and vaporized material "squirt" from the edges of the projectile's contacts which form an ejecta blanket and potentially secondary craters. The distance the ejecta (and secondary craters) travel is based primarily upon the target body's gravity and the impactor's velocity. However, recent work suggests that terrain may also play a role in this, at least in the extent and distribution of secondary craters (Robbins and Hynes, 2011d, or Section 4.2).

The third and final stage of crater formation is modification, not to be confused with the modification discussed in Section 1.4.2. Though one can argue the modification phase progresses through geologic time until the crater is destroyed, this usually refers to the main collapse phase. The main collapse is dominated by the target's gravity, but the local properties of

the crust will influence this process (*e.g.*, Pike, 1980; Boyce *et al.*, 2006; Robbins and Hynek, 2011c). This phase begins after the crater is fully excavated and is still a simple bowl shape. Loose debris slide down the interior walls of smaller craters, further-widening them and causing them to grow shallower. Large craters will form complex morphology: large chunks of the wall collapse forming terraces, and a rebound effect causes central peak(s) or a ring to rise. One or more rings form if the rebound that forms the peak "overshoots" the stability of the rock, at which point it collapses back into a ring (this is the same phenomenon observed in simple milk drop experiments). Over a much greater timescale in larger craters (but still generally instantaneous in a geologic context), isostatic rebound causes the floor to rise and flatten, further departing from a bowl morphology.

The timescale for each phase is instantaneous in a geologic sense; it is this relative rapidity that allows craters to be important tools for understanding global stratigraphic relationships (see Section 1.4.1). The initial compression phase lasts  $\tau_{\text{compression}} = L/v_i$ , where  $L$  is the diameter of the impactor and  $v_i$  its velocity. The ~40-50-meter projectile that likely formed the ~1.2-km-diameter Meteor Crater in Arizona, USA thus spent a small fraction of a second in this stage. The excavation stage is dependent upon the diameter  $D$  of the crater and gravity  $g$  of the impacted object,  $\tau_{\text{excavation}} = \sqrt{D/g}$ , so Meteor Crater took ~10 seconds to excavate. The modification stage will take a few times that of the excavation, so overall, Meteor Crater, a ~1.2-km-diameter feature, took under 1 minute to form. In comparison, the large, 222-km-diameter crater Lyot on Mars took ~10-15 minutes to form, while the giant 2500-km South Pole-Aitken basin on the Moon may have taken ~2 hours.

### **1.3. Basic Crater Properties and Morphologies**

Craters range in size from micrometer-scale zap pits or microcraters (as seen on lunar samples) to giant basins thousands of kilometers in diameter (*e.g.*, South Pole-Aitken Basin (2500 km) and Mare Imbrium (1123 km) on the Moon; Caloris Basin (1350 km) on Mercury; and Utopia (3300 km) and Hellas (2300 km) on Mars). Despite spanning over nine orders of

magnitude in size, all craters form with the same three basic characteristics: A cavity below the surrounding surface, a raised rim above the surrounding surface, and ejected material surrounding the rim. This assumed basic morphology aids in the study of craters because deviation from this basic model is indicative of subsequent modification or properties of the formation of the crater itself.

Within those three basic characteristics, crater morphology changes significantly based upon crater size. The size-morphology classification can be broken down into three main categories: simple, complex, and multi-ring basin. The transition diameter at which a crater will form as simple vs. complex is primarily proportional to  $g^{-1}$ , where  $g$  is the surface gravity of the target body (*e.g.*, Gilbert, 1893; Pike, 1988). However, the transition between these types does not occur at an exact diameter for a given planetary surface: Not all craters smaller than 6 km are simple just as not all craters larger than 6 km are complex on Mars. First, it is dependent upon the type of morphology being examined (*i.e.*, while central peaks and wall terraces are both characteristics of complex craters, central peaks on Mars are prevalent in craters with diameters  $D \geq 5.6$  km, but terraces at  $D \geq 8.3$  km (Robbins and Hynek, 2011c, see Section 3.6.2)). Second, it is dependent upon the physical properties of the crust in which it formed; the primary factor is the strength of the crust for smaller craters and strength and thickness of the underlying lithosphere for multi-ring basins (*e.g.*, McKinnon and Melosh, 1980; Pike, 1980; Melosh, 1989).

Simple craters are a bowl-shaped depression below the surface with a raised rim and surrounding ejecta blanket (until the latter two may be removed through erosion). (See Appendix C for examples of crater morphologies.) Meteor Crater in Arizona and the crater Linné on the moon are classic examples of simple craters. Simple craters' cavities are steepest at the rim and gradually shallow in slope until the center is reached. Simple craters have no lower diameter limit, but they do have an upper limit: For the Moon, simple craters are generally craters smaller than ~15 km (Pike, 1977, 1988), while on Mars, the transition between simple and complex morphologies is generally between 5 and 8 km (Pike, 1980, 1988; Boyce and Garbeil, 2007; Robbins and Hynek, 2011c), though simple craters as large as 15 km have been

observed (Robbins and Hynek, 2011c).

Complex craters display distinctly different internal morphology than simple craters. Instead of a gentle bowl-shaped cavity, complex craters have sloping walls that terminate in a mostly flat floor. Nearly all pristine, complex craters have outwardly slumping terraced walls. These terraces are observed to trap impact melt (rock that was melted due to the energy of a hypervelocity impact) which indicates they formed during the initial crater formation as opposed to subsequent mass wasting (Melosh, 1989). The smallest complex craters usually have a peak in the center that is composed of material below the floor that was uplifted through an elastic rebound effect. This is much like the rebound when a small object is dropped into a pool of water (Melosh, 1989). Central peaks have been observed to rise above the surface outside the crater (*e.g.*, crater Theophilus on the Moon, various craters on Mars (Robbins and Hynek, 2011b)), though it is rare to have them higher than the rim itself. Somewhat larger complex craters display a central ring as opposed to a peak; the transition diameter to a ring also scales as  $g^{-1}$ . A transition to this peak ring morphology on the Moon is seen in craters generally larger than  $\sim 140$  km (Melosh, 1989). This transition on Mars is significantly more difficult to discern because only nine craters display this morphology (all are  $D > 100$  km except one), despite over 300 craters being  $D > 100$  km. Given that the majority of these larger craters formed early in Mars' history and have undergone significant modification (Robbins and Hynek, 2011b), this is likely due predominantly to erosion processes removing the peak rings.

Multi-ring basins are historically considered the largest craters and are generally more difficult to recognize due to their size and age. On the Moon, basins are the next size-based morphologic type beyond the peak-ring type of complex craters (*e.g.*, Mare Orientale on the Moon), though it is less apparent that this is the case for large basins on other bodies (*e.g.*, Caloris on Mercury, Argyre and Hellas on Mars (see Section 3.2.1), and Valhalla on Callisto). Melosh (1989) argues that these basins are dissimilar to lunar multi-ring basins and, even if some can be shown to be of the lunar type, the transition diameter to this morphology does not appear to scale inversely with gravity; this indicates their formation and collapse mechanism is different

than that of simple and complex craters. He does, however, emphasize that the basic basin morphology - a very large (hundreds to thousands of kilometers) diameter, relatively shallow depth (~few kilometers), and various ring-like collapse features - is the largest observed type of crater. Basins have an added effect: Because they are so large, the energies required to form them can also cause dramatic tectonic effects to manifest across the entire body. For example, at the antipode to Caloris Basin on Mercury, the terrain is chaotic in nature with faults and significantly modified craters, suggesting vertical jostling by several kilometers (Spudis and Guest, 1988). On Mars, the antipode to Argyre basin is the Elysium volcanic complex and the antipode to Hellas basin is the Tharsis volcanic complex, though a causal as opposed to coincidental link between these has yet to be confirmed.

Another feature of many craters is that they produce secondary craters during formation. These are formed by blocks of material thrown from the planetary surface during the excavation phase of impact. These blocks are ejected with a range of angles and velocities, impact the surface, and create their own smaller, shallower craters. Due to the ballistic nature of ejecta, they often form in chains that are oriented radially to the primary crater or have biaxially symmetric morphologies with a long axis radial to the primary (Shoemaker, 1962, 1965). The ejected material has much slower velocities than the initial impact, and so the secondary craters will usually not be the radially symmetric simple type. Due to energy conservation, secondary craters will always be smaller than primary craters, typically less than 5% the diameter of the primary and more often less than 2.5% (McEwen and Bierhaus, 2006). However, in rare cases secondary craters as large as 15% of the primary have been suggested (Robbins and Hynek, 2011d).

#### **1.4. The Utility of Craters in Understanding Planetary Processes**

Because of the universal crater properties and established impact history in the inner solar system (Fig. 1), craters are an important tool for understanding terrestrial bodies. One can examine craters individually to discern local processes (*e.g.*, aeolian deposition, fluvial erosion, lower crust composition), or one can study a large group of craters to learn about a broad region

of a planet's surface, ages, and variations within properties of the crust. Similarly, laboratory experiments of impacts can be scaled to larger sizes only so much before they break down, so studies of large craters across the solar system allow tests of models and experiments and can lead to new avenues of research.

#### ***1.4.1. Relative Surface Ages***

There are two basic premises behind using craters to age-date a surface: (1) The longer a surface is exposed, the more craters accumulate upon it, and (2) over geologic time, craters are distributed randomly on a planet. With these simple assumptions, one can count how many craters are on one surface vs. another to determine which is older: Older surfaces have more craters over a given area. Taking this a step further, one can separate the counted craters into diameter size bins to create a size-frequency distribution (SFD) crater plot (c.f., Arvidson *et al.*, 1979). The histogram can be integrated from the largest diameter to the smallest, such that the smallest diameter bin will contain the sum of all the craters observed (cumulative SFD). A feature of these cumulative SFDs is that on logarithmic axes the distribution of cumulative number of craters vs. diameter sizes is approximately linear, mirroring the production function if no crater removal processes have taken place. Since a surface will collect more craters as it ages (assuming no other processes take place to remove them), isochrons can be established for reference in dating surfaces of a certain age (an isochron is an idealized, modeled curve on a SFD that represents what the crater distribution should be for a surface of a given age from that model). This is generally based significantly upon models extrapolated from the Moon (the most recent comprehensive works are: Ivanov, 2001; Neukum *et al.*, 2001; Hartmann and Neukum, 2001; Hartman, 2005).

That is the first major limitation of crater-based surface ages: Crater counting itself can only yield *relative* ages. It is possible to estimate surface ages based upon present-day observed craters, and this has been attempted and refined many times for Mars throughout the last ~40 years (*e.g.*, Chapman and Jones, 1977; Ivanov, 2001; Hartmann and Neukum, 2001; Hartmann,

2005). This is less of a limitation on the Moon because the *Apollo 12* and *14-17* missions returned samples of the lunar regolith and rocks from different-aged surfaces, and these rocks were subsequently dated via radiometric methods ( $\text{Rb}^{87}/\text{Sr}^{87}$  and  $\text{U}^{238}/\text{Pb}^{206}$ ) (e.g., Heiken *et al.*, 1991; Stöffler and Ryder, 2001). Geologic mapping of the moon via stratigraphic relationships, volcanic flows, and impact crater density permits categorization of the lunar surface into distinct groups based on similar features and ages. The major lunar epochs are based upon major impact events because impacts occur in a geologic instant and a large enough impact has effects that can be traced a large distance from the site. For example, the most recent lunar epoch is the Copernican, covering the time since Copernicus crater formed  $\sim 1$  Ga ago (the others from most recent to oldest are Eratosthenian, Imbrian, Nectarian, and Pre-Nectarian) (Stöffler and Ryder, 2001). Copernicus has a large ejecta blanket and rays that extend a significant distance from the crater rim that permit stratigraphy to be established over a large portion of the lunar surface. By following these kinds of features and correlating them with crater densities, each part of the surface can be assigned a relative age date. These can then be calibrated with the *Apollo* returns and assigned absolute ("actual") ages. Efforts have since been made (e.g., Hartmann and Neukum, 2001; Ivanov, 2001; Hartmann, 2005) to extrapolate the cratering rate from the Moon to Mars to better constrain Martian chronology.

A second limitation involves sheer number statistics: The smaller the number of craters counted, the larger the statistical uncertainties. Uncertainties on crater SFDs are the square-root of the number in each bin (Arvidson *et al.*, 1979). This is because craters are distinct features - one crater is one crater - so they follow Poisson statistics where the standard deviation from the mean  $N$  is  $\sqrt{N}$ . Therefore, when attempting to date one region relative to another, it behooves the investigator to utilize as many craters as possible. Unfortunately, this is not always viable, such as when attempting to date a small region, a young region, and/or when using low-resolution data.

A third difficulty is repeatability: One researcher counting craters in a region will not necessarily count the same number for a given diameter range as another. They may not even

count the same number as they did the last time they attempted it. Hartmann *et al.* (1981) and Lissauer *et al.* (1988) estimate that uncertainties based upon this alone will generally introduce an uncertainty of a factor of  $1.2-1.3\times$ , while this researcher found differences of  $>4\%$  (Robbins *et al.*, 2011) and Kirchoff *et al.* (2011) found differences on the few-percent level. Similarly, solar illumination angle will affect crater counts: If the sun is too close to the meridian when the image was taken, crater shadows will not be long enough to make them easily identifiable. Experimental results with the same terrain imaged at different incidence angles suggest the ideal angle range is  $\sim 70-80^\circ$  (*e.g.*, Wilcox *et al.*, 2005; Ostrach *et al.*, 2011).

The fourth main difficulty in using craters to age-date surfaces is that of saturation. While a surface ages, it will accumulate more craters: a cumulative size-frequency plot will have a slope of  $b \approx -3$ . However, this is only true to a point. Beyond a given crater density, no new craters will be able to form without erasing an equivalent area of existing craters. At this time, no new information can be gleaned from craters of that size since the number per bin will no longer increase. Because smaller craters accumulate more quickly than larger craters, smaller craters will become saturated first. The slope on a cumulative SFD when saturated is  $b \approx -1.8$ , but it is usually approximated as  $b \approx -2$  (*e.g.*, Hartmann, 2005).

There are two different types of saturation - one is theoretical and the other is what happens on a real planetary body. First, geometric saturation is the theoretical saturation of a surface when craters are arranged in a honey comb-like hexagonal closest-packing, such that the maximum number possible may be emplaced without overlap. Since, in theory, an infinite number of craters could be emplaced if one continued to shrink their size, a practical limit was placed upon the derivation where two orders of magnitude would be considered part of a hexagonal pack. It was found that in this case, the number of (saturated) craters of a given diameter is  $N_s = 1.54D^{-2}$  (Gault and Wedekind, 1978). The second, practical type is "equilibrium," sometimes referred to as "empirical saturation." This is the practical limit when craters are deposited randomly on a planetary body. Experiments by Gault and Wedekind (1978) showed that when randomly deposited, craters would reach equilibrium at 1-10% of geometric

saturation, with 5-7% being the mean. No planetary surface comes close to geometric saturation; the closest known is on Mimas, and it is only for craters 10-20 km in diameter that equilibrium is as large as 13% of geometric saturation (Melosh, 1989).

The fifth and final main complicating factor involves secondary craters. Secondary craters were first problematized a half century ago (Shoemaker, 1962) and, while further work was done over the years (*e.g.*, Shoemaker, 1965; Oberbeck and Morrison, 1974; Wilhelms *et al.*, 1978), the issue was generally ignored by the planetary community until recent years with a pair of papers (Bierhaus *et al.*, 2005; McEwen *et al.*, 2005). Their work showed that secondary craters can indeed confound planetary ages and crater statistics over large portions of the surface. Despite 50 years of study, secondary craters remain a relative enigma in terms of secondary crater SFD (*e.g.*, McEwen and Bierhaus, 2006; Ong *et al.*, 2011; Robbins and Hynek, 2011d), where secondary craters will be emplaced relative to the primary (*e.g.*, Lucchitta, 1977; Schultz and Singer, 1980; McEwen and Bierhaus, 2006; Preblich *et al.*, 2007; Robbins and Hynek, 2011a, 2011d), or even a model that can predict if secondary craters will be produced in abundance or paucity from a primary impactor. There is no solid model for how these form nor for their properties, so they must be taken into account on an individual basis by individual researchers, some of whom doubt their existence (*e.g.*, Neukum *et al.*, 2006) or influence (*e.g.*, Hartmann, 2007). Generating large global databases of craters with features complete down to small sizes is therefore an important step in understanding secondary craters: They begin to allow detailed studies of secondary craters in a uniform, global, and terrain-dependent manner (Robbins and Hynek, 2011d, or Section 4.2).

#### ***1.4.2. Modification Effects on Craters***

As a surface accumulates craters, the craters themselves will be emplaced according to a production function with slopes of  $b \approx -3$  on a log-log cumulative size-frequency graph during the present day (various lines of evidence suggest this has changed throughout time, *e.g.*, Strom *et al.* (2008)). It will continue to accumulate craters until it reaches an equilibrium point, at

which time no new craters can be deposited of that size range, and the slope will turn over to  $b \approx -2$ . However, this only occurs if there are no other processes affecting the craters. On airless bodies such as the Moon and Mercury, this is not usually a complicating factor; on Mars (and to a much greater extent, Earth), it is the *de facto* case, and craters' modification and removal yield important clues to the planet's history.

Physical weathering is an important geologic process that acts to move material from a higher elevation to a lower one or transport it in general. Impact craters themselves are the simplest weathering that occurs on all planetary surfaces. These both destroy the surface in which the crater formed and deposit a blanket of ejecta in the surrounding terrain. The gravitationally driven process of mass wasting will also affect craters on all bodies (not to be confused with the modification stage of crater formation, discussed above). The effects will be a general lowering of the crater's uplifted rim and infilling of the crater floor from rim material, outside material, and wall material that has slumped, rolled, or fallen in.

The addition of a substantive atmosphere (Venus, Earth, Mars, and Titan) will greatly speed the weathering process, not only because wind itself will transport suspended material, but also because it will drive particles along the ground (creep) and transport them via saltation. Adding a low-viscosity liquid (*e.g.*, liquid water (Earth, Mars) or ethane (Titan)) increases the weathering rate again because of the sheer increase of mass: Liquids are much denser than gases under most circumstances, and so a flowing liquid will carry much more kinetic energy, allowing it to transport or erode a proportionally larger amount of material. High-viscosity fluids (*e.g.*, lava on Venus, Earth, Moon, and Mars) will result in even higher rates of erosion due to the greater kinetic energy; in a practical sense, lava will more likely cover and bury a region as opposed to carry and deposit material from one place to another. On bodies with temperatures close to the triple point of a molecule (*e.g.*, H<sub>2</sub>O on Earth and Mars, C<sub>2</sub>H<sub>6</sub> on Titan), thermal erosion will also play a role where the melting of permafrost will dramatically weaken the rock and can lead to collapse or more rapid erosion through the processes discussed above. The general effects of endogenic weathering on the size-frequency crater population are to remove

craters, and it is more likely to remove smaller craters than larger ones because smaller craters are shallower. For this latter process, studying partially buried impact craters can show the depth of lava burial, but this is only the case if one knows *a priori* what the original crater depth should have been, requiring regional studies into crater depth-diameter relationships (see Section 3.5).

The modification processes mentioned above (impacts, mass wasting, erosional, and burial) are the main ones that will modify the existing crater population on Mars. As a crater is modified, the depth will decrease and the crater diameter will increase; estimates are that the crater diameter can grow by up to 30% (*e.g.*, Melosh, 1989; Craddock, *et al.*, 1997; Craddock and Howard, 2002). Lacking a raised rim at this point, it is much easier to transport material (aeolian and fluvial deposition) into the crater cavity, and it will eventually reach the point where it is completely filled (Craddock, *et al.*, 1997), although it may still be detectable via subtle albedo differences or a topographic depression (Frey, 2006, 2008; Robbins and Hynek, 2011b).

These alteration mechanisms will affect a local surface uniformly (*e.g.*, Chapman and Jones, 1977), so a smaller crater will "feel" the effects of erosion more easily than a large crater. For this reason, it is possible to estimate the erosion or deposition rates based upon the smallest crater size that differs from a production or equilibrium crater population. For example, if there is an erosion rate of 1  $\mu\text{m}/\text{yr}$  and craters 1 m-deep are emplaced once every 1 Ma, then the surface will have a significant deficit of  $\lesssim 1$  m-deep craters because they will be eroded at the same rate they form. One km-deep craters, meanwhile, would be much less affected. For this reason, the small impactor population and frequency of impact is open to much more interpretation than the larger ones: (1) The small crater population is more easily eroded so it is more difficult to compare with an expected production function, (2) the production function is poorly defined at smaller diameters because observing small solar system objects and determining a census is limited by their visibility, and (3) compounding effects of secondary craters at these diameters confuse the crater census and add further uncertainty to comparison with observed impactor populations.

If one assumes these issues have a minimal effect or can be well modeled and accounted

for in the analysis, then the erasure effect also can be used to roughly determine major erosive events at various locations through time. For example, Mars' highlands have a significant deficit of craters  $5 \lesssim D \lesssim 30$  km (*e.g.*, Chapman and Jones, 1977; Barlow, 1988; Robbins and Hynek, 2011b). Craters smaller than this are in production. This is interpreted to mean Mars suffered a substantial erosive event in its early history that resulted in the removal of many of those craters (*e.g.*, Chapman and Jones, 1977; Craddock and Maxwell, 1993) or it had a different production function at that time (*e.g.*, Barlow, 1988). By examining the morphology of the individual craters and the surfaces around them, it is thought that fluvial processes cause most of the erosion (*e.g.*, Craddock and Maxwell, 1993; Craddock and Howard, 2002). The erosion cut-off time can be estimated based upon what crater sizes are in production, since it will take longer to accumulate craters 1 km across than craters 1 m across.

#### ***1.4.3. Types of Crater Distribution Graphs***

From the above discussion, the size-distribution of craters on a planetary surface can inform a researcher of numerous processes that have occurred both on the surface and to the impactor population. To analyze these, there are three different types of graphs that can be generated from crater data that only require knowing the diameters of the craters. These are crater "size-frequency distributions" (SFDs) (see Arvidson *et al.*, 1979). The three types of SFDs are incremental SFDs (ISFDs), cumulative SFDs (CSFDs), and R-plots (relative plots). Except for specialized applications, such as database comparison, all SFDs should be normalized to the surface area on which the craters were identified. Crater SFDs fundamentally follow a power-law distribution, where there are many more smaller craters in a population for a given number of larger craters. For this reason, SFDs are displayed on log-log axes. Examples of these three types for the same two regions of the planet Mars are shown in Fig. 2; the regions show a relatively young section of Mars centered around Utopia Basin (25-45°N, 110-150°E) and a comparatively old portion of the Martian southern highlands (25-45°S, 140-180°E). The areas of each are the same,  $2.3 \times 10^6$  km<sup>2</sup>.

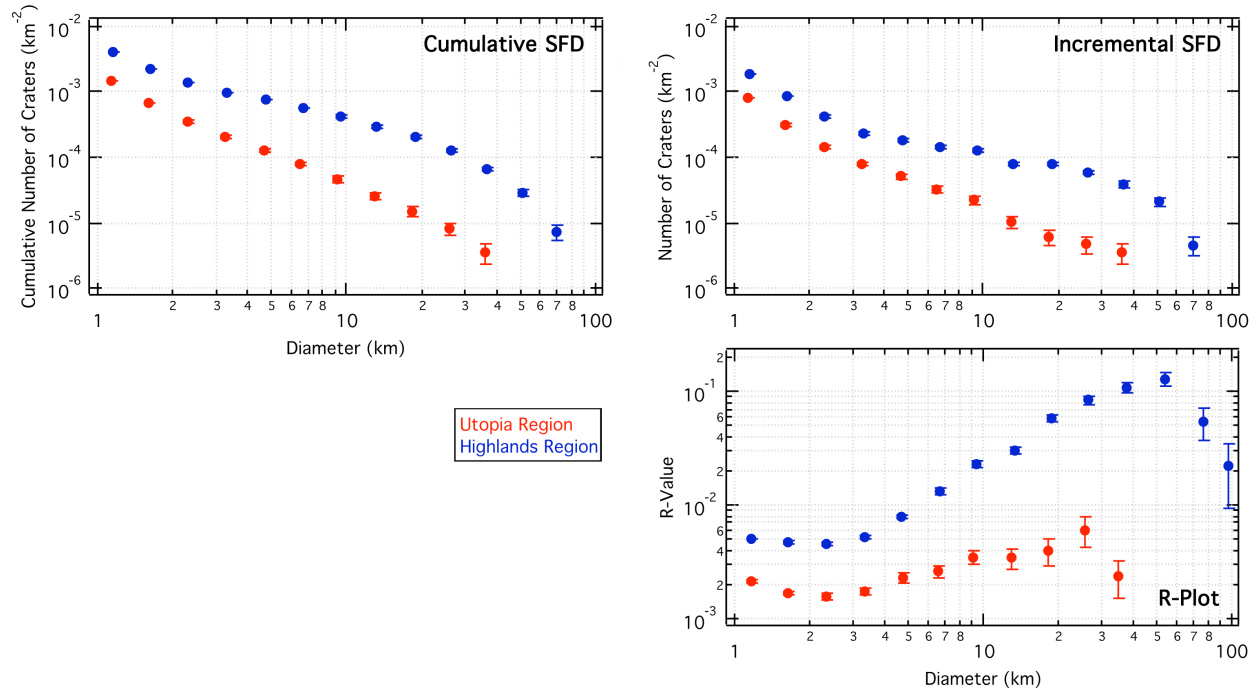


**Figure 2:** Examples of incremental, cumulative, and R-plots size-frequency distributions of the same two areas of Mars.

ISFDs are, at their core, a histogram of craters where the diameter is plotted on the abscissa and number of craters per diameter bin are displayed on the ordinate. The diameters are binned such that they are evenly spaced on the horizontal axis. The common diameter interval is  $D$  to  $\sqrt{2}D$  (Arvidson *et al.*, 1979). Individual researchers may vary this interval depending upon the range and number of craters in their data, but they will usually do so in integers  $N$  of the  $D$  to  $\sqrt[N]{2}D$  range and not have coarser binning than recommended by Arvidson *et al.* (1979).

CSFDs are generated usually as a derivation from an ISFD. The data from the ISFD are integrated (discretely summed because the data are not continuous) from larger diameters through smaller diameters such that the smallest diameter bin contains all craters within the sample region. CSFDs are much more common in the literature than ISFDs and it is for these types of plots that crater isochrons are usually calculated. An alternative method of generating a CSFD is to sort the craters from largest to smallest diameter bin and then display diameters on the abscissa and row number on the ordinate since the row number will be the sum of the number of all craters larger than it. Because CSFDs are - by nature - cumulative, their values at smaller

diameters are resolution-independent.

Both ISFDs and CSFDs show that craters usually follow a simple power-law distribution. Production functions on a CSFD from present-day cratering rates typically have slopes  $b \approx -3$ , while cratering during the Heavy Bombardment and LHB have been shown to probably follow different slope distributions (*e.g.*, Barlow, 1988; Strom *et al.*, 2008). Examining crater populations for deviations from the expected slopes are the most common use of these kinds of plots, but many researchers find them unsuitable for ready visual inspection of these differences.

Hence, the R-plot SFD type can be used. This is a type of ISFD where the data are normalized to a  $b = -3$  slope such that a crater population with an ISFD  $b = -3$  slope will be a horizontal line. Similar to the other types, the horizontal axis contains crater diameter and the diameter bins are again in intervals from  $D$  to  $\sqrt{2}D$ . The value  $R$  is calculated from Eq. 1:

$$R = \frac{\bar{D}^3 N}{A(D_b - D_a)} \quad (1)$$

where  $\bar{D}$  is the geometric mean of the diameters of the craters between  $D_a$  and  $D_b$  or, if these are unavailable, then the diameter bin boundaries ( $\bar{D} \approx \sqrt{D_a D_b}$ );  $N$  is the number of craters in the diameter bin,  $A$  is the surface area of the region in which craters are identified, and the diameter bins are  $D_a < D_b$  (Arvidson *et al.*, 1979).

Different groups of researchers each prefer different SFD types. When comparing results with other groups, one must be cognizant of this. For example, W.K. Hartmann (*e.g.*, Hartmann (2005)) prefers the ISFD display. His isochron work (Hartmann, 2005) is determined for an ISFD and so when using the Hartmann isochrons, one must use the ISFD type plot. Alternatively, G. Neukum (*e.g.*, Neukum *et al.*, 2001) prefers CSFD plots and so when utilizing that group's isochrons and comparing with their data (*e.g.*, Neukum *et al.*, 2001), one must also use a CSFD. Meanwhile, other researchers, such as Strom (*e.g.*, Strom *et al.*, 2008) and Chapman (*e.g.*, Chapman *et al.*, 2002) prefer R-plots. It is generally recommended that at least an R-plot and ISFD or CSFD are displayed for the same data in publications (Arvidson *et al.*, 1979), though this recommendation is rarely followed.

## **1.5. The Importance of Detailed Crater Catalogs**

The above discussion details the formation process of impact craters, their basic properties, and uses. While this discussion is fundamental to understanding craters and their importance, its utility is severely diminished without actually having craters in a catalog or database to study (both terms – catalog and database – are used interchangeably throughout this document). Uniformly generated crater databases from a single method and a single researcher or group are fundamental to using craters for a diverse range of investigations – from better understanding the impact process to age dating to discerning the properties across the planetary surface upon which they are emplaced.

Combining different groups' catalogs can lead to biases within the metacatalog, as discussed above and estimated by Hartmann *et al.* (1981) and Lissauer *et al.* (1988) to be a factor of  $\sim 1.2-1.3\times$ . This basic concept formed one of the core justifications for compiling the original *Catalog of Large Martian Impact Craters* (Barlow, 1988) and its revision (Barlow, 2003), and it was a prime factor in generating global catalogs since (*e.g.*, Stepinski *et al.*, 2009; Salamunićcar *et al.*, 2011; Robbins and Hynek, 2011b, 2011c). Inclusion of more and smaller craters permits more detailed studies to be done, allowing detailed stratigraphy and age relationships (*e.g.*, Tanaka *et al.*, 2011), as well as broad, uniform studies of secondary crater characteristics and relationships relative to their primaries (Robbins and Hynek, 2011d).

Detailed morphologic and morphometric data significantly assist in the above tasks. At a fundamental level, characterizing the interior morphology of craters results in the formulation of basic scaling laws discussed above (Section 1.3) and below (Section 3.6). Morphometric information about crater topography (depth, rim height, etc.) permits testing of fundamental scaling laws of crater depth-to-diameter ratios (Section 3.5). Once these have been established for a fresh crater population (requiring crater degradation/modification state (see Section 2.4.4)), changes among fresh crater depth-to-diameter ratios can be used to track different strengths of the planet's crust (Section 3.5.1), and different infilling/erosion rates across the surface (Section 3.2.5). Observations of ejecta blanket morphology from the first Mars flyby missions identified

cohesive, layered ejecta blankets on Mars not previously observed in the solar system and only now found on Mars, Ganymede, and Europa (see Barlow *et al.*, 2000, and references therein) (Section 3.3.3.1). Careful morphologic classifications included in a global database allow for craters to be studied in a uniform, global way and, when combined with morphometric properties, permits testing of formation hypotheses.

Put concisely, the broad, fundamental importance of impact crater databases is: They allow detailed, uniform studies of planetary surfaces, applicable to a wide variety of diverse and important applications from predicting effects bombs and missiles to planning for planetary catastrophes to basic science research. To fulfill the potential of modern data for allowing this work on Mars, I have manually compiled the largest database to-date of impact craters on a single body: the planet Mars in this case. The craters number 631,333 in total and 378,540 with diameters  $D \geq 1$  km. In this dissertation, I explain how I generated the database (Section 2) and a broad overview of its characteristics and a re-examination of classic scaling laws (Section 3) that will serve as a basis for future investigations. I then use the database to investigate some of the properties of secondary craters (Section 4). Finally, I delve deeper into the use of small craters, where I identified an additional  $\sim 100,000$  craters within volcanic calderas and used them to partially reconstruct the history of volcanism across the planet (Section 5) in one of the most common applications of impact crater counting.